

Gauged Flavor Group with Left-Right Symmetry

Diego Guadagnoli^a, Rabindra N. Mohapatra^b and Ilmo Sung^b

^a *Laboratoire de Physique Théorique, Université Paris-Sud, Centre d'Orsay, F-91405 Orsay-Cedex, France*

^b *Maryland Center for Fundamental Physics, Department of Physics, University of Maryland, College Park, MD 20742, USA*

Email: diego.guadagnoli@th.u-psud.fr, rmohapat@umd.edu, sung@umd.edu

(Dated: November 4, 2018)

ABSTRACT: We construct an anomaly-free extension of the left-right symmetric model, where the maximal flavor group is gauged and anomaly cancellation is guaranteed by adding new vectorlike fermion states. We address the question of the lowest allowed flavor symmetry scale consistent with data. Because of the mechanism recently pointed out by Grinstein *et al.* tree-level flavor changing neutral currents turn out to play a very weak constraining role. The same occurs, in our model, for electroweak precision observables. The main constraint turns out to come from W_R -mediated flavor changing neutral current box diagrams, primarily $K - \bar{K}$ mixing. In the case where discrete parity symmetry is present at the TeV scale, this constraint implies lower bounds on the mass of vectorlike fermions and flavor bosons of 5 and 10 TeV respectively. However, these limits are weakened under the condition that only $SU(2)_R \times U(1)_{B-L}$ is restored at the TeV scale, but not parity. For example, assuming the $SU(2)$ gauge couplings in the ratio $g_R/g_L \approx 0.7$ allows the above limits to go down by half for both vectorlike fermions and flavor bosons. Our model provides a framework for accommodating neutrino masses and, in the parity symmetric case, provides a solution to the strong CP problem. The bound on the lepton flavor gauging scale is somewhat stronger, because of Big Bang Nucleosynthesis constraints. We argue, however, that the applicability of these constraints depends on the mechanism at work for the generation of neutrino masses.

Contents

1. Introduction	1
2. Flavor Symmetry within Left-Right Models	3
3. Phenomenology	7
3.1 Tree-level FCNC effects	8
3.2 Loop FCNC effects and lower bound on the W_R mass	9
3.3 Flavor gauge boson mass scale	11
3.4 Fermion mixing and its consequences	11
3.4.1 Electroweak precision tests	14
3.4.2 The decay $\bar{B} \rightarrow X_s \gamma$	17
3.5 Further constraints	18
3.5.1 Electric dipole moments	18
3.5.2 Top quark flavor changing effects	18
3.5.3 Direct searches	18
4. Lepton Sector	19
4.1 Neutrino masses	19
4.2 Constraints	19
5. Conclusions	21

1. Introduction

One of the long-standing mysteries of physics beyond the Standard Model is the origin of flavor patterns for quarks and leptons. In the Standard Model (SM), they arise from the quark and lepton Yukawa couplings with the SM Higgs boson and are arbitrary, thereby precluding any physical insight as to their origin. Since these flavor patterns may well be the remnants of the breaking of some symmetry, the belief is that pinning down the flavor symmetry at work could provide hints of the underlying dynamics at work. Many possibilities for approaching this important issue from the vantage point of symmetry then present themselves – starting from discrete non-abelian subgroups of these flavor symmetries to continuous global or local ones. The question then arises as to how we determine by low energy observations which particular mechanism is at work and at which scale such a symmetry manifests itself. The hope is that different choices will lead to different characteristic predictions, e.g. a global horizontal symmetry would lead to massless

familons at low energies [1] and discrete symmetries could lead to some relations between observables.

A widely discussed possibility is to study gauged flavor symmetries [2], which leads to a number of interesting effects such as new gauge bosons and new flavor changing effects mediated by these bosons. The very first test of this possibility is to determine the scale of gauged flavor symmetry. Naïve considerations seem to suggest that this scale is likely to be in the 1000 TeV range; however in specific models this expectation could change drastically. For example, in a recent paper by Grinstein, Redi and Villadoro (GRV) [3], it has been shown by explicit construction that there are SM extensions with gauged flavor symmetry where this scale could be in the 1 TeV range or even below, compatible with constraints from the hadronic sector. Furthermore this model predicts, by the requirement of anomaly cancellation, new vectorlike quarks, the lightest of which with masses again in the TeV ballpark, hence within the reach of LHC direct searches. The mechanism at work in the GRV model is an inverse, see-saw like, relation between the masses of the quarks and those of the new fermion states [4] as well as of the flavor gauge bosons, so that the partners of the heaviest quarks are the lightest among the new states. This fact allows to pass all the flavor changing neutral current (FCNC) constraints in a very natural way.

A certain degree of model dependence in the idea of gauging the flavor symmetry is the choice of new fermionic states added in order to cancel the gauge anomalies. To achieve this, the simplest option is to include new, vectorlike quark partners. This choice may however appear to be at odds with that of quark states that need sit in chiral representations. This simple consideration motivates us to pursue here an alternative possibility, where the maximal gauging of flavor symmetry is carried out within a left-right symmetric extension of the SM [5]. This implies that the flavor symmetry group is itself left-right symmetric. The new gauge anomalies resulting from the larger gauge group cancel with the introduction of vectorlike new fermionic partners of the quarks [4]. Besides the known virtues inherent in left-right symmetric extensions of the SM, e.g. the possibility to justify the hypercharge quantum numbers, there appear to be the following advantages in our approach: *(i)* it provides a natural way to include neutrino masses; *(ii)* in the quark Lagrangian, it features only three free parameters in the gauge and Yukawa sector, after the rest are fixed by data on quark masses and mixings; *(iii)* the model provides a simple solution to the strong CP problem without the need for an axion, in a manner similar to that discussed in Refs. [6,7].

There are two possible realizations of this idea while keeping the gauge group to be $SU(2)_L \times SU(2)_R \times U(1)_{B-L}$ at the TeV scale: *(a)* the discrete parity symmetry is maintained down to the TeV scale or *(b)* it is broken at some very high scale [8] so that, at the TeV scale, the two gauge couplings as well as the left and right Yukawa couplings are in general different from each other. We will consider both alternatives below. Within the second alternative, the solution to the strong CP problem mentioned above is not obvious.

Concerning the constraints on the model outlined above, we find that, similarly as in the GRV model, tree-level FCNCs mediated by the flavor gauge bosons are tamed automatically by the hierarchy of their masses. Also, in our case, electroweak (EW) precision tests are automatically fulfilled in the bulk of the parameter space.

The strongest constraint comes from W_R -mediated FCNC box diagrams, primarily

$K - \bar{K}$ mixing. The implied bounds on the scale of the new vectorlike quarks as well as on the flavor gauge bosons, which will be discussed in detail in secs. 3.2, 3.3 and 3.4, depend however on the scale at which parity is broken.

Compatibly with these bounds, the new effects, accessible at the current generation of TeV hadron colliders, include the lightest among the new particles' masses and various deviations in top-physics observables, like top production and decays. Such deviations are due to the fact that the top (in particular, the right-handed one) mixes non-negligibly onto its new fermionic partner, whereas mixing is tiny to absent for the rest of the quark states. This in turn explains why no deviations are to be expected in the production or decays of any other quark than t_R .

For an overview of the organization of this paper we refer the reader to the table of content on page 1.

2. Flavor Symmetry within Left-Right Models

In the SM, once the Yukawa couplings are set to zero, the maximal flavor symmetry group is $SU(3)_{Q_L} \times SU(3)_{u_R} \times SU(3)_{d_R} \times SU(3)_{\ell_L} \times SU(3)_{\ell_R}$. If the weak gauge group is extended to that of the left-right symmetric model, the flavor group becomes $SU(3)_{Q_L} \times SU(3)_{Q_R} \times SU(3)_{\ell_L} \times SU(3)_{\ell_R}$ which is more economical and, unlike the SM, also simultaneously explains neutrino masses.¹

We will therefore start with the gauge group $G_{LR} \equiv SU(3)_c \times SU(2)_L \times SU(2)_R \times U(1)_{B-L} \times SU(3)_{Q_L} \times SU(3)_{Q_R} \times SU(3)_{\ell_L} \times SU(3)_{\ell_R}$, where $SU(3)_{Q_L} \times SU(3)_{Q_R}$ represents the flavor gauge symmetries respectively in the left- and right-handed quark sector, and $SU(3)_{\ell_L} \times SU(3)_{\ell_R}$ the corresponding ones for the lepton sector. The particle content and its transformation properties under fundamental representations of the group G_{LR} are reported in table 1. One can clearly note the one-to-one correspondence between the quark and the lepton multiplets, differing only in the behavior under $SU(3)_c$. It is easy to verify that this field content makes G_{LR} completely anomaly-free, separately in the quark and lepton sectors.

We next discuss the quark Yukawa couplings. We will ignore for the moment the leptonic ones since they do not have any effect on the final results for the quark sector. (The leptonic flavor symmetries are discussed in sec. 4.) In writing the quark Lagrangian at the TeV scale, we will generally assume that the gauge symmetry $SU(2)_L \times SU(2)_R \times U(1)_{B-L}$ is restored at that scale. Even under this assumption, one has still to specify where the parity symmetry is broken. As anticipated in the Introduction, one can either suppose that parity is restored at the TeV scale, or else that its restoration takes place at some much higher scale M_P [8]. Let us first focus on the former case, namely of TeV-scale parity. In this case, the Lagrangian for the quark sector reads

$$\begin{aligned} \mathcal{L}_q = & \mathcal{L}_q^{\text{kin}} - V(Y_u, Y_d, \chi_L, \chi_R) + \lambda_u(\bar{Q}_L \tilde{\chi}_L \psi_R^u + \bar{Q}_R \tilde{\chi}_R \psi_L^u) + \lambda_d(\bar{Q}_L \chi_L \psi_R^d + \bar{Q}_R \chi_R \psi_L^d) \\ & + \lambda'_u \bar{\psi}_L^u Y_u \psi_R^u + \lambda'_d \bar{\psi}_L^d Y_d \psi_R^d + \text{h.c.} , \end{aligned} \quad (2.1)$$

¹For other horizontal symmetry extensions of left-right models, see [9]. Furthermore, gauged flavor symmetries have also been discussed in the context of the Pati-Salam GUT in ref. [10], see appendix therein.

	$SU(2)_L$	$SU(2)_R$	$U(1)_{B-L}$	$SU(3)_{Q_L}$	$SU(3)_{Q_R}$	$SU(3)_c$	$SU(3)_{\ell_L}$	$SU(3)_{\ell_R}$
Q_L	2		$\frac{1}{3}$	3		3		
Q_R		2	$\frac{1}{3}$		3	3		
ψ_L^u			$\frac{4}{3}$		3	3		
ψ_R^u			$\frac{4}{3}$	3		3		
ψ_L^d			$-\frac{2}{3}$		3	3		
ψ_R^d			$-\frac{2}{3}$	3		3		
L_L	2		-1				3	
L_R		2	-1					3
ψ_L^e			-2					3
ψ_R^e			-2				3	
ψ_L^ν			0					3
ψ_R^ν			0				3	
χ_L	2		1					
χ_R		2	1					
Y_u				$\bar{3}$	3			
Y_d				$\bar{3}$	3			
Y_ℓ							$\bar{3}$	3
Y_ν							$\bar{3}$	3

Table 1: Model content. For ease of readability, horizontal lines separate the quark multiplets, the lepton ones and the Higgs and flavon ones from each other, and only non-singlet transformation properties are reported explicitly.

where we have written explicitly only the Yukawa interactions. We note at this point that, since under parity $Q_L \leftrightarrow Q_R$ and $\psi_L^u \leftrightarrow \psi_R^u$ (and similarly for $\psi_{L,R}^d$), parity symmetry requires $Y_{u,d} \leftrightarrow Y_{u,d}^\dagger$ and the $\lambda_{u,d}$ as well as $\lambda'_{u,d}$ couplings to be real.² Parity will thus be broken only by the different vevs of $\chi_{L,R}$ (the tilde on these fields in eq. (2.1) indicates $\tilde{\chi} = \tau_2 \chi^*$ for both L and R).

In the case where parity is broken at a scale M_P much higher than the TeV [8], the interactions in eq. (2.1), obtained from each other by the parity operation defined in the previous paragraph, have in principle different couplings. For example

$$\lambda_u(\bar{Q}_L \tilde{\chi}_L \psi_R^u + \bar{Q}_R \tilde{\chi}_R \psi_L^u) \rightarrow \lambda_{uL} \bar{Q}_L \tilde{\chi}_L \psi_R^u + \lambda_{uR} \bar{Q}_R \tilde{\chi}_R \psi_L^u, \quad (2.2)$$

because of different RGE running beneath the scale M_P . Hence, similarly as in eq. (2.2), in the case of no TeV-scale parity we will distinguish the left and right instances of each gauge, λ and λ' couplings by an L or R subscript.

²In particular, concerning $\lambda_{u,d}$, one can note that there is one single such coupling for either of the up-type or down-type quark interactions with heavy fermions. Hence, one can remove possible phases in $\lambda_{u,d}$ by absorbing them in the ψ^u and ψ^d fields, respectively.

Concerning the breaking of the gauge groups, the flavor gauge group $SU(3)_{Q_L} \times SU(3)_{Q_R}$ is broken spontaneously by the vevs of Y_u and Y_d while the group $SU(2)_L \times SU(2)_R$ by the vevs of the Higgs doublets, $\chi_{L,R}$, as already mentioned. In particular, we adopt the following vev normalization

$$\langle \chi_L \rangle = \begin{pmatrix} 0 \\ v_L \end{pmatrix}, \quad \langle \chi_R \rangle = \begin{pmatrix} 0 \\ v_R \end{pmatrix}, \quad (2.3)$$

while diagonal Y vevs will be denoted henceforth as $\langle \hat{Y}_{u,d} \rangle$.

Fermion masses

From eq. (2.1) one can read off the up-type fermion mass Lagrangian to be $\mathcal{L}_m = \bar{\mathcal{U}}_L M_u \mathcal{U}_R$, with $\mathcal{U} = \text{column}\{u, \psi^u\}$, each of the u and ψ^u fields carrying a generation index. The mass matrix reads

$$M_u = \begin{pmatrix} 0 & \lambda_u v_L \mathbb{1}_{3 \times 3} \\ \lambda_u v_R \mathbb{1}_{3 \times 3} & \lambda'_u \langle \hat{Y}_u \rangle \end{pmatrix}, \quad M_d = \begin{pmatrix} 0 & \lambda_d v_L \mathbb{1}_{3 \times 3} \\ \lambda_d v_R \mathbb{1}_{3 \times 3} & \lambda'_d \langle \hat{Y}_d \rangle \end{pmatrix}. \quad (2.4)$$

For the time being, we assume the parameters $\lambda_u v_L$ and $\lambda_u v_R$ to be much smaller than any of the $\lambda'_u \langle \hat{Y}_u \rangle_i$. (With the subscript i in $\langle \hat{Y}_{u(d)} \rangle_i$ we shall henceforth label the diagonal entries of the flavon vev matrices.) Then, to leading order in an expansion in the parameters $\frac{\lambda_u v_{L(R)}}{\lambda'_u} \langle \hat{Y}_u \rangle_i^{-1}$, and analogous for the down sector, the above mass matrices assume the following diagonal form

$$\hat{M}_u \simeq \begin{pmatrix} \frac{\lambda_u^2 v_L v_R}{\lambda'_u \langle \hat{Y}_u \rangle} & 0 \\ 0 & \lambda'_u \langle \hat{Y}_u \rangle \end{pmatrix}, \quad \hat{M}_d \simeq \begin{pmatrix} \frac{\lambda_d^2 v_L v_R}{\lambda'_d \langle \hat{Y}_d \rangle} & 0 \\ 0 & \lambda'_d \langle \hat{Y}_d \rangle \end{pmatrix}. \quad (2.5)$$

From eq. (2.5) it is evident that off-diagonalities in the light-quark Yukawa couplings are inherited from off-diagonalities in the flavon vevs $\langle Y_{u,d} \rangle$. We note first that, even below the v_L scale, it is always possible to have one of the flavon vevs in diagonal form through an appropriate redefinition of the $\psi_{L,R}^u$ and $\psi_{L,R}^d$ basis (see eq. (2.1)). We choose Y_d to be that particular flavon multiplet. This amounts to three parameters, fixed by the down-type quark masses. Y_u will then be chosen to have a vev pattern of the form

$$\langle Y_u \rangle = V_R^\dagger \langle \hat{Y}_u \rangle V_L, \quad \langle Y_d \rangle = \langle \hat{Y}_d \rangle, \quad (2.6)$$

with $V_{L,R}$ unitary. Note that, as already mentioned, $V_L = V_R = V$ in eq. (2.6) follows from the $\langle Y_u \rangle$ vev pattern being hermitian and hence parity symmetric. This amounts to six real parameters and three phases. Two of these phases can be absorbed as relative phases of two up-type quark fields relative to the third one. This gives the six real parameters and one phase to fit up-type quark masses and the CKM matrix.³

³We also note incidentally that, from the point of view of our discussion, the $\lambda'_{u,d}$ couplings can in principle be absorbed into the definition of the $Y_{u,d}$ vevs respectively. This effectively leaves as free parameters only $\lambda_{u,d}$, besides the scale of the vev v_R and the $SU(2)_R$ coupling g_R , making the model very economical.

In the basis of eq. (2.6), and again in the temporary approximation $v_R \ll \langle \hat{Y}_{u,d} \rangle$, the Yukawa couplings of the SM (defined from the interactions $\bar{u}_L y_u u_R$ and $\bar{d}_L y_d d_R$) read

$$y_u = \frac{\lambda_u^2 v_R}{\lambda'_u} V_L^\dagger \langle \hat{Y}_u \rangle^{-1} V_R, \quad y_d = \frac{\lambda_d^2 v_R}{\lambda'_d} \langle \hat{Y}_d \rangle^{-1}. \quad (2.7)$$

One can now rotate the $u_{L,R}$ fields as

$$u_{L(R)} = V_{L(R)}^\dagger \hat{u}_{L(R)}, \quad d_{L(R)} = \hat{d}_{L(R)}. \quad (2.8)$$

In the hatted basis, y_u is diagonal and V_L is moved to the $\bar{u}_L \gamma^\mu W_\mu d_L$ interaction. Therefore, V_L can be interpreted as the CKM matrix, V_{CKM} . As already stated, in our case of left-right symmetry we have strictly $V_L = V_R = V$ at the scale v_R . However, since we are interested only in v_R values not very far from the electroweak symmetry breaking scale v_L , the radiative corrections to the above relation between left and right CKM's are expected to be small. Therefore, we will henceforth generally identify

$$V_L = V_R = V_{\text{CKM}}, \quad (2.9)$$

with caveats to be commented upon more below in the analysis. Since quark masses are given by $y_i v_L$, we can draw some conclusions from the approximate relations (2.7):

- (i) In the limit of $v_R \ll \langle \hat{Y}_{u,d} \rangle_i$ the elements of the diagonal $\langle \hat{Y}_{u,d} \rangle$ matrices follow an inverted hierarchy with respect to the quark masses [3, 4].
- (ii) For a given value of v_R and of the $\lambda^{(i)}$ couplings, eqs. (2.7) or the corresponding exact expressions in sec. 3.4 allow to univocally fix the $\langle \hat{Y}_{u,d} \rangle$ entries. Since the $Y_{u,d}$ vevs set also the mass scale for the flavor gauge bosons (see below in this section for details), the inverted hierarchy mentioned in item (i) implies a similar hierarchy in new flavor changing neutral current effects: the lighter the generations, the more suppressed the effects [3]. This is arguably one of the most attractive features of the model. We will return to this quantitatively in sec. 3.1.
- (iii) In the exact parity case, the mass matrices $M_{u,d}$, see eq. (2.4), lead to $\arg \det[M_{u,d}] = 0$, implying that the strong CP parameter at the tree level vanishes. The one loop calculation for a more general case of this type was carried out in Ref. [7]. Using this result, we conclude that the model solves the strong CP problem without the axion.

Since the condition $v_R \ll \langle \hat{Y}_{u,d} \rangle_i$ may in general not hold for all flavors, we need to give for the quark masses a more exact relation than eq. (2.5). In fact, the fermion mixing matrices (2.4) can be diagonalized exactly. This will be discussed in sec. 3.4, along with its phenomenological consequences.

Flavor gauge boson masses

The masses of the $SU(3)_{Q_L} \times SU(3)_{Q_R}$ gauge bosons $G_{iL,R}$ ($i = 1, \dots, 8$) are obtained from the kinetic terms of Y_u and Y_d in the Lagrangian, $\text{Tr}(|D^\mu Y_{u,d}|^2)$, where the covariant derivatives are

$$D^\mu Y_{u,d} = \partial^\mu Y_{u,d} - ig_H G_R^\mu Y_{u,d} + ig_H Y_{u,d} G_L^\mu. \quad (2.10)$$

The relevant mass terms read

$$\begin{aligned}\mathcal{L} &= \text{Tr} (|g_H G_R^\mu \langle Y_u \rangle - g_H \langle Y_u \rangle G_L^\mu|^2) + \text{Tr} (|g_H G_R^\mu \langle Y_d \rangle - g_H \langle Y_d \rangle G_L^\mu|^2) \\ &= \frac{1}{2} \mathcal{G}_k (M_V^2)_{kl} \mathcal{G}_l ,\end{aligned}\tag{2.11}$$

where $\mathcal{G}_k \equiv \{G_L^a, G_R^a\}$ is a vector containing the 16 fields in $G_{L,R}^\mu = G_{L,R}^{\mu a} \frac{\lambda^a}{2}$. The \mathcal{G}_k are rotated by an orthogonal matrix O such that $\mathcal{G}_k = O_{kj} \hat{\mathcal{G}}_j$, where $\hat{\mathcal{G}}_i$ are mass eigenstates.

One interesting point to note is that all the flavor gauge boson masses are determined by basically only one Y vev, namely the largest of the Y_u vevs $\langle \hat{Y}_u \rangle_1$. In fact, for the lightest among the $M_{\mathcal{G}_i}$, $\langle \hat{Y}_u \rangle_1$ is multiplied by two powers of the Cabibbo angle θ_C (in the limit $\theta_C \rightarrow 0$, one gets at least one massless \mathcal{G}_i) and $\langle \hat{Y}_u \rangle_1 \times \theta_C^2$ is larger than the second-largest Y vev contribution, $\langle \hat{Y}_u \rangle_2$.

3. Phenomenology

In the subsections of this section we will discuss the various observables that are expected to provide a constraint (or else the possibility of a signal) for the model. Since in some cases – starting from the model spectrum – the model predictions vary in a wide range, we found it useful to explore these predictions with a flat scan of the model parameters. In the case where parity is assumed to be restored at the TeV scale, ranges have been chosen as follows:

1. $g_H \in [0.3, 0.9]$ and v_R such that $M_{W_R} \in [0.2, 5]$ TeV (the bound on M_{W_R} from applicable constraints is taken into account afterwards).
2. $\lambda_u \in [0.96, 5]$, $\lambda_d \in [0.1, 5]$, see discussion below eq. (3.9).
3. Setting the couplings $\lambda'_{u,d} = 1$, one effectively absorbs them into the definition of the $Y_{u,d}$ vevs, respectively (the relevant combination entering fermion mixing is $\lambda'_{u,d} Y_{u,d}$, see eqs. (2.4)). This assumption is however restrictive for the mass spectrum of the flavor gauge bosons, that depends on $\langle \hat{Y}_{u,d} \rangle$, but not on $\lambda'_{u,d}$, see eq. (2.11). Therefore, we have also scanned $\lambda'_{u,d} \in [0.1, 5]$.
4. Finally, we have taken $g_L = g_R \simeq 0.65$ for the $SU(2)_{L,R}$ couplings.

In the other scenario where parity is not a good symmetry at the TeV scale, all the left vs. right couplings can be chosen as different from each other. Concerning the $SU(2)_{L,R}$ couplings, in [8] examples have been given of scenarios where $g_R/g_L \sim 0.70$ for a UV complete theory which conserves parity. Here we therefore limit ourselves to the reference choice $g_R = 0.7 \cdot g_L$. Concerning the other parameters:

- The left and right instances of the g_H and $\lambda'_{u,d}$ couplings have been scanned in the same ranges as specified in items 1 and 3 respectively.
- With regards to item 2, we have scanned $\lambda_{uL} \in [0.96, 5]$ and the rest of the λ parameters in $[0.1, 5]$.

- We have further enforced that the left vs. right instances of each coupling do not differ from each other by more than a factor of 5.

Two concluding comments concern the reality of the $\lambda^{(\prime)}$ couplings and the hermiticity of the Yukawa vevs, implicitly assumed in the above items. From the discussion below eq. (2.1), one can argue that, in the case where parity is not a good TeV-scale symmetry, non-negligible complex phases may be present in (some of) the $\lambda^{(\prime)}$ couplings. This may in turn have an impact on CP violating observables, which are, however, not the main concern in this paper, for the reasons mentioned in sec. 3.2. Finally, departures from hermiticity in the Yukawa vevs correspond (see discussion beneath eq. (2.6)) to assuming sensible departures from eq. (2.9). Throughout this paper we neglect such effects. Again, we will comment on this assumption in sec. 3.2.

3.1 Tree-level FCNC effects

The flavor gauge bosons $G_{L,R}^{\mu a}$ couple to the currents $\mathcal{J}_{HL,R}^{\mu a} \equiv g_H \bar{Q}_{L,R} \gamma^\mu \frac{\lambda^a}{2} Q_{L,R}$. Similarly as in Ref. [3], these interactions give rise to new, tree-level, contributions to the 4-fermion operators

$$\begin{aligned} Q_1^{q_j q_i} &= (\bar{q}_i^\alpha \gamma_L^\mu q_j^\alpha) (\bar{q}_i^\beta \gamma_{\mu,L} q_j^\beta) , \\ \tilde{Q}_1^{q_j q_i} &= Q_1^{q_j q_i} |_{L \rightarrow R} , \\ Q_5^{q_j q_i} &= (\bar{q}_i^\alpha P_L q_j^\beta) (\bar{q}_i^\beta P_R q_j^\alpha) , \end{aligned} \quad (3.1)$$

with Latin and Greek indices on the quark fields denoting flavor and respectively color, and where $P_{L,R} \equiv (1 \mp \gamma_5)/2$. In the quark mass eigenstates basis, the Wilson coefficients of the above operators read

$$\begin{aligned} C_1^{q_j q_i} &= -\frac{g_H^2}{8} (M_V^2)_{a,b}^{-1} (V_L^q \lambda^a V_L^{q\dagger})_{ij} (V_L^q \lambda^b V_L^{q\dagger})_{ij} , \\ \tilde{C}_1^{q_j q_i} &= -\frac{g_H^2}{8} (M_V^2)_{8+a,8+b}^{-1} (V_R^q \lambda^a V_R^{q\dagger})_{ij} (V_R^q \lambda^b V_R^{q\dagger})_{ij} , \\ C_5^{q_j q_i} &= \frac{g_H^2}{2} (M_V^2)_{a,8+b}^{-1} (V_L^q \lambda^a V_L^{q\dagger})_{ij} (V_R^q \lambda^b V_R^{q\dagger})_{ij} , \end{aligned} \quad (3.2)$$

where q can be u or d , and a sum over a and b in the range $1, \dots, 8$ is understood. The matrices $V_{L,R}^{u,d}$ rotating the u, d fields from the flavor to the mass eigenbasis should be chosen as

$$V_{L,R}^u = V_{L,R} , \quad V_{L,R}^d = \mathbb{1} , \quad (3.3)$$

compatibly with eq. (2.8) and in the approximation of neglecting the mixing between quarks and heavy fermion states.

Updated bounds on the Wilson coefficients in eq. (3.2) have been reported by the UTfit collaboration [11] and usefully tabulated in their table 4 for the different meson-antimeson mixing processes. The contributions, predicted in our model, to the above coefficients have been explored by the random scan mentioned at the beginning of sec. 3. As previously anticipated, these contributions are well within the existing bounds in the bulk of the

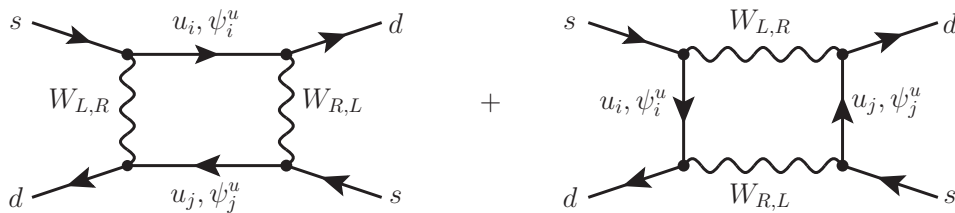


Figure 2: Box diagrams contributing to the $K_L - K_S$ mass difference in our model.

explored parameter space. As an illustration, we report in Fig. 1 the *largest* in magnitude among these contributions, that to the $K - \bar{K}$ mixing coefficient $\text{Re}(C_K^5)$, in the case of TeV-scale parity. The M_{W_R} mass is therefore mostly bounded from box diagrams with W_R exchange, as discussed in sec. 3.2. The resulting bound, $M_{W_R} \gtrsim 2.5$ TeV [12], is shown in Fig. 1 as a vertical shaded area extending leftwards. On the M_{G_i} masses, on the other hand, we will return in sec. 3.3.

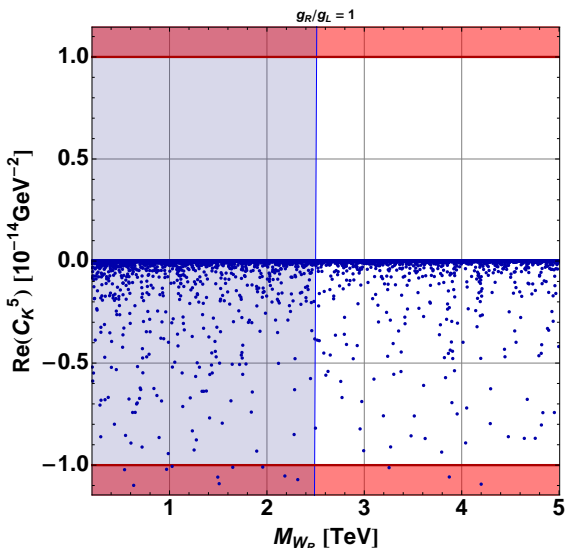


Figure 1: M_{W_R} vs. the contribution to the $\Delta F = 2$ Wilson coefficient $\text{Re}(C_K^5)$. The horizontal (red) shaded regions are excluded from the analysis of Ref. [11]. The vertical (blue) region extending leftwards is the M_{W_R} bound from loop FCNCs [12].

First note that the upper fermion line in any of the box diagrams of Fig. 2 will be proportional to a factor of $V_R^\dagger \cos(\theta_{i,R}^u) m_i^u \cos(\theta_{i,L}^u) V_L$ or $V_R^\dagger \sin(\theta_{i,R}^u) M_i^u \sin(\theta_{i,L}^u) V_L$ depending on whether the fermion is a quark or its heavy fermionic partner (in the lower fermion lines one will have the hermitian conjugate of the same expressions). Assuming propagation of a single quark species, it is therefore easy to see that ΔM_K is such that

$$\Delta M_K \propto g_L^2 g_R^2 \left| V_R^\dagger c_{i_R} c_{i_L} \left(\frac{m_i}{p^2 - m_i^2} - \frac{t_{i_R} M_i t_{i_L}}{p^2 - M_i^2} \right) V_L \right|_{12}^2, \quad (3.4)$$

⁴Even more stringent bounds would come from CP violating observables again in the K sector, but these bounds are much more model dependent [13].

3.2 Loop FCNC effects and lower bound on the W_R mass

In ref. [12], it was pointed out that box diagrams with mixed W_L -quark and W_R -quark exchange provide a severe lower bound on the $SU(2)_R$ -symmetry breaking scale in the case of the minimal LR symmetric model with Higgs bidoublets. This happens on account of the constraint from the $K_L - K_S$ mass difference, ΔM_K , and the bound reads $M_{W_R} \gtrsim 2.5$ TeV.⁴

In our model, beside the known quarks, also their heavy fermionic partners propagate in the box diagrams, because of fermion mixing. The full amplitude, for a given quark-heavy fermion doublet (e.g. t and $\psi_{u,3}$), is depicted in Fig. 2. The sum of the contributions turns out to display a GIM-like mechanism of cancellation, as we will shortly explain.

where we have abbreviated \cos, \tan with c, t and dropped the superscript on the masses. One should note at this point that

- a. the mass eigenvalues for quarks and heavy fermions come with opposite signs (cf. eq. (2.4)),
- b. m_i and $t_{i_R} M_i t_{i_L}$ are equal, as can be seen by using eqs. (3.8), namely that the generally small mixing angles are compensated by a large mass in the second term in the parenthesis of eq. (3.4),
- c. after factoring out the common mass term mentioned in item b, the diagram is proportional to $m_i^2 - M_i^2$, as in the GIM mechanism. In our model the mass difference between a quark and its fermionic partner is smallest in the top sector. Interestingly, in most of the meson mixings' phenomenology of the down-sector, including the CP violating observable ϵ_K , the top contribution is the most important one.

The observation in item c has the potential of substantially weakening the severe bounds on the parity breaking scale coming from ϵ_K [12], and we reserve to come back to this issue in a separate study. As stated elsewhere, the predictions for CP violating observables are however quite model-dependent, and here we confine our discussion to CP conserving ones, in particular ΔM_K . In this case, the dominant loop contribution comes from the charm sector, hence the mechanism described above is much less effective, since the quark - heavy fermion splitting is very large. On account of this constraint, we find that the lower bound on the W_R mass from $K_L - K_S$ mass difference coincides with that in ref. [12], namely we get $M_{W_R} \gtrsim 2.5$ TeV. This bound holds in the exact parity case ($g_R/g_L = 1$), that we have been assuming in this discussion.

On the other hand, if parity is broken at a scale much higher than the TeV scale, one expects a splitting in the TeV-scale values of g_L and g_R in eq. (3.4), and values of $(g_R/g_L)^2 < 1$ provide a further suppression of eq. (3.4) by the same factor. For example, assuming $g_R/g_L = 0.7$, this bound scales down to $M_{W_R} \gtrsim 1.7$ TeV. One can see this by simply noting that, as far as M_{W_R} and the $SU(2)_{L,R}$ gauge couplings are concerned, ΔM_K scales as $\Delta M_K \propto g_L^2 g_R^2 / M_{W_R}^2$, and that the ΔM_K calculation in the SM is dominated by loops mediated by the charm quark, whose vectorlike partner ψ_2^u is, to first approximation, decoupled. As discussed at the beginning of sec. 3 the choice $g_R/g_L = 0.7$ [8] will be our reference one for the scenario of no TeV-scale parity.

Two further comments are in order here. First, we note that a choice such as $g_R/g_L = 0.7$ will also affect the W_R collider bound since the W_R production rate will go down by the factor $(g_R/g_L)^2$ as well. Second, high-scale parity breaking will in general also cause some misalignment of the left and right CKM matrices. In particular, large off-diagonal entries in the right CKM matrix have the potential of correspondingly increasing the contributions to flavor observables, a simple example being, again, that of meson anti-meson mixings. The interest of this example is in the fact that the potential phenomenology of these

contributions encompasses not only flavor violation, but also *mixing*-induced CP violation, namely observables like $|\epsilon_K|$, $\sin 2\beta$ and $\sin 2\beta_s$.⁵

For the aims of the present discussion, we will assume that CKM entries undergo corrections due to RGE that don't modify their hierarchical structure, hence that the induced misalignment between V_L and V_R is small enough not to grossly alter the main argument of this section. A more detailed answer can be given, we feel, only in the context of specific models.

3.3 Flavor gauge boson mass scale

As mentioned above, from the point of view of flavor violating effects mediated by \mathcal{G}_i exchange, the model is compatible with $M_{\mathcal{G}_i}$ as small as $O(\text{TeV})$, and this represents a potentially interesting new signal. Of course the question arises here, whether there are other model constraints placing a more stringent lower bound on this mass.

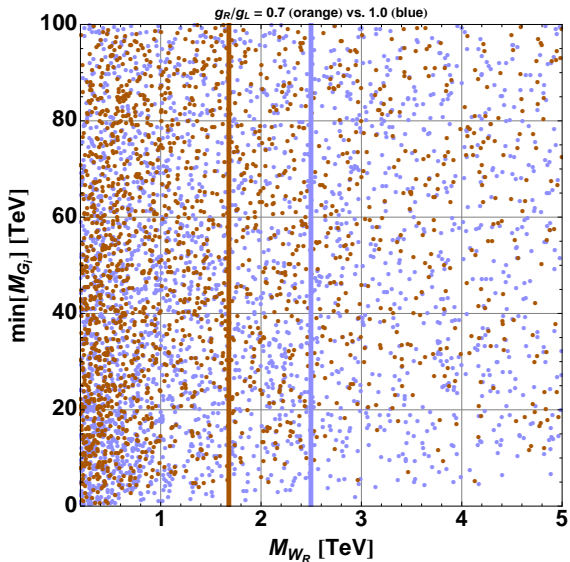


Figure 3: M_{W_R} vs. the mass of the lightest flavor gauge boson, $\min(M_{\mathcal{G}_i})$, for $g_R/g_L = 0.7$ (orange dots) or 1.0 (blue dots).

in the two cases of exact TeV-scale parity (meaning $g_R/g_L = 1$) and of no TeV-scale parity (where we assume, as mentioned $g_R/g_L = 0.7$ [8]). From the lowermost points, one can see that the minimum $M_{\mathcal{G}_i}$ mass tends to grow with growing M_{W_R} . In particular, the lowermost red (blue) points on the right of the red (blue) vertical line imply allowed $M_{\mathcal{G}_i}$ values going down to about 3 TeV.

3.4 Fermion mixing and its consequences

The fermion mixing matrix M_u in eq. (2.4) can be diagonalized via orthogonal transfor-

⁵On the other hand, we do not expect large effects to these observables to come from the other potential sources of flavor mixing discussed in this paper, namely tree-level FCNCs mediated by flavor gauge bosons (see sec. 3.1) or quark – heavy-fermion mixing (see sec. 3.4.2).

mations acting separately on each generation i and each chirality, namely:

$$\begin{pmatrix} \hat{u}_i \\ \hat{\psi}_i^u \end{pmatrix}_{L(R)} = \mathcal{R}(\theta_{L(R),i}^u) \begin{pmatrix} u_i \\ \psi_i^u \end{pmatrix}_{L(R)}, \quad \text{with } \mathcal{R}(\theta) \equiv \begin{pmatrix} \cos \theta & -\sin \theta \\ \sin \theta & \cos \theta \end{pmatrix}, \quad (3.5)$$

where the hats denote mass eigenstates. This eigenvalue problem admits the following analytic solution (we recall again that the diagonal entries of the flavon vev matrices are denoted with $\langle \hat{Y}_{u(d)} \rangle_i$)

$$(m_{u,i}^\pm)^2 = \frac{1}{2} \left((\lambda'_u \langle \hat{Y}_u \rangle_i)^2 + \lambda_u^2 (v_L^2 + v_R^2) \pm \Delta_i^u \right),$$

$$\text{with } \Delta_i^u \equiv \sqrt{(\lambda'_u \langle \hat{Y}_u \rangle_i)^4 + 2(\lambda'_u \langle \hat{Y}_u \rangle_i)^2 \lambda_u^2 (v_L^2 + v_R^2) + \lambda_u^4 (v_L^2 - v_R^2)^2} \quad (3.6)$$

with rotation angles given by

$$\tan \theta_{L,i}^u = \frac{\lambda_u^2 (v_L^2 - v_R^2) - (\lambda'_u \langle \hat{Y}_u \rangle_i)^2 + \Delta_i^u}{2\lambda_u v_L \lambda'_u \langle \hat{Y}_u \rangle_i},$$

$$\tan \theta_{R,i}^u = \frac{\lambda_u^2 (v_R^2 - v_L^2) - (\lambda'_u \langle \hat{Y}_u \rangle_i)^2 + \Delta_i^u}{2\lambda_u v_R \lambda'_u \langle \hat{Y}_u \rangle_i}. \quad (3.7)$$

Provided the λ, λ' couplings are of the same order, we will generally have $(\lambda_u v_L)^2 \ll (\lambda_u v_R)^2, (\lambda'_u \langle \hat{Y}_u \rangle_i)^2$. Accordingly expanding the above formulae one obtains the following approximate, but accurate solution ($x_i \equiv (\lambda_u v_L / \lambda'_u \langle \hat{Y}_u \rangle_i)^2$)

$$(m_{u,i}^-)^2 = \frac{\lambda_u^4 v_L^2 v_R^2}{\lambda_u^2 v_R^2 + (\lambda'_u \langle \hat{Y}_u \rangle_i)^2} + \mathcal{O}(x_i^2), \quad (m_{u,i}^+)^2 = \lambda_u^2 v_R^2 + (\lambda'_u \langle \hat{Y}_u \rangle_i)^2 + \mathcal{O}(x_i),$$

$$\tan \theta_{L,i}^u = \frac{\lambda_u v_L \lambda'_u \langle \hat{Y}_u \rangle_i}{\lambda_u^2 v_R^2 + (\lambda'_u \langle \hat{Y}_u \rangle_i)^2} + \mathcal{O}(x_i^{3/2}), \quad \tan \theta_{R,i}^u = \frac{\lambda_u v_R}{\lambda'_u \langle \hat{Y}_u \rangle_i} + \mathcal{O}(x_i). \quad (3.8)$$

Here m^- and m^+ are to be identified respectively with the quark and heavy partners masses. A completely analogous solution exists in the down sector and is obtained from the above formulae with just the substitution $u \rightarrow d$. Note that the quark masses implied by the approximate $y_{u,d}$ in eq. (2.7) can be obtained from the $m_{u,i}^-$ in eq. (3.8) in the limit $\lambda_u v_R \ll \lambda'_u \langle \hat{Y}_u \rangle_i$.

Let us focus on the general solution in eqs. (3.6) and (3.7). For fixed λ_u and v_R , one can determine the combination $\lambda'_u \langle \hat{Y}_u \rangle_i$ by inverting the equations $m_{u,i=1,2,3}^- = m_{u,c,t}$, with the up-type quark mass values on the r.h.s. These equations admit a real solution in $\lambda'_u \langle \hat{Y}_u \rangle_i$ only for sufficiently high λ_u . Note in fact that, with fixed values for the other parameters, the maximum of $(m_{u,i}^-)^2$ occurs for $\lambda'_u \langle \hat{Y}_u \rangle_i = 0$ (see also the first of eqs. (3.8)). Necessary condition for a real solution to exist is therefore

$$m_{u,c,t} < m_{u,i}^-(\lambda'_u \langle \hat{Y}_u \rangle_i = 0)|_{i=1,2,3} = \lambda_u v_L, \quad (3.9)$$

where we have assumed $v_L < v_R$. Since $v_L \simeq 174$ GeV – very close to m_t – the above inequality implies $\lambda_u \gtrsim 0.94$. (From the analogous inequalities in the down-quark sector, one also derives $\lambda_d \gtrsim 0.02$.) Note as well that, for the boundary value $\lambda_u = 0.94$, the solution of eq. (3.9) for $i = 3$ is $\lambda'_u \langle \hat{Y}_u \rangle_3 = 0$. This explains the lower bound chosen for λ_u in our scans, see beginning of sec. 3.

Parity-broken case

In the case where parity is not a good symmetry at the TeV scale, we would expect the light quark Yukawa couplings to be left-right asymmetric as already noted. In this case, the formulae for quark as well as heavy-fermion masses and mixings change accordingly, i.e. eqs. (3.8) are replaced by

$$\begin{aligned} (m_{u,i}^-)^2 &= \frac{\lambda_{uL}^2 \lambda_{uR}^2 v_L^2 v_R^2}{\lambda_{uR}^2 v_R^2 + (\lambda'_u \langle \hat{Y}_u \rangle_i)^2} + O(x_i^2), & (m_{u,i}^+)^2 &= \lambda_{uR}^2 v_R^2 + (\lambda'_u \langle \hat{Y}_u \rangle_i)^2 + O(x_i), \\ \tan \theta_{L,i}^u &= \frac{\lambda_{uL} v_L \lambda'_u \langle \hat{Y}_u \rangle_i}{\lambda_{uR}^2 v_R^2 + (\lambda'_u \langle \hat{Y}_u \rangle_i)^2} + O(x_i^{3/2}), & \tan \theta_{R,i}^u &= \frac{\lambda_{uR} v_R}{\lambda'_u \langle \hat{Y}_u \rangle_i} + O(x_i). \end{aligned} \quad (3.10)$$

This case becomes very similar to the GRV examples [3] and as we see from the figures below allows vectorlike quark masses of about 2 TeV, making them, in principle, accessible at the LHC. If $\lambda_{u(d)R} \ll \lambda_{u(d)L}$, then the vectorlike quark masses could be even lighter, as is clear from eq. (3.10).

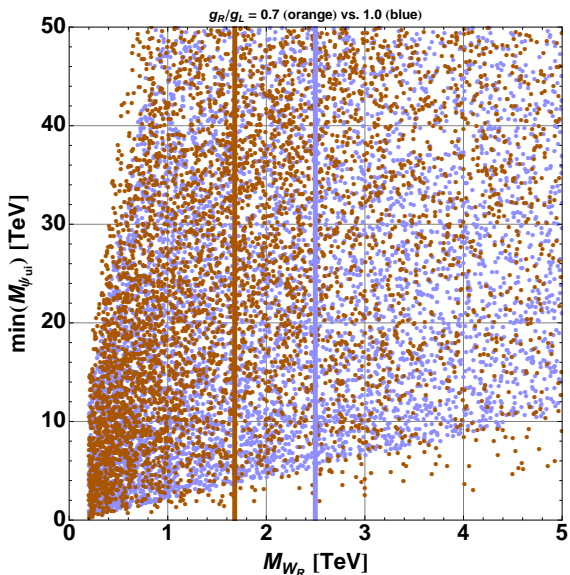


Figure 4: M_{W_R} vs. the mass of the lightest (up-type) fermionic partner, for $g_R/g_L = 0.7$ (orange dots) or 1.0 (blue dots). The vertical lines – again in orange or blue for $g_R/g_L = 0.7$ or 1 – represent the M_{W_R} bound discussed in sec. 3.2.

$m_{d,i}^+$ solutions in eq. (3.8). According to these equations, the heavy fermion masses are correlated with both the $SU(2)_R$ -breaking scale v_R and with the scales of gauge flavor symmetry breaking. In practice the latter correlation is blurred by the dependence on the unknown λ and λ' parameters. On the other hand, the correlation with v_R still allows to infer the lowest allowed values for $M_{\psi_i^u}$ and $M_{\psi_i^d}$, taking into account the M_{W_R} bound discussed in sec. 3.2. The situation is illustrated in Fig. 4, that displays the lightest up-type fermion partner mass vs. M_{W_R} . Blue and respectively orange dots refer to the

The one difference from the TeV-scale parity case is that there is no reason for $\lambda'_{u,d}$ to be real and therefore the model does not solve the strong CP problem. However, if there is parity restoration at some high scale, at that scale one does have a solution to the strong CP problem and an extrapolation is necessary to estimate how large a θ is induced at low energy. This kind of analysis is beyond the scope of this paper and we hope to take it up separately.

Bounds on heavy-fermion masses and mixings

The interesting phenomenological question is that of the magnitude of the mixing angles and of the lowest allowed masses $M_{\psi_i^u}$ and $M_{\psi_i^d}$ for the heavy up-type and down-type fermion partners. Note that these masses are given by the $m_{u,i}^+$ and

parity vs. no-parity scans, see beginning of sec. 3 for details. The vertical lines represent the corresponding M_{W_R} bounds. One can see that, while the exact parity case seems to exclude $M_{\psi_i^u} \lesssim 5$ TeV, in the no parity case masses going down to 2 TeV or even lower are possible. We mention that we found similar values to be possible also for the lightest down-type heavy fermion masses. In fact, as evident already from the first of eqs. (3.8), a large m_t/m_b ratio does not necessarily imply a corresponding hierarchy in $\lambda'_d \langle \hat{Y}_d \rangle_3 / \lambda'_u \langle \hat{Y}_u \rangle_3$ because $\lambda_u^4 / \lambda_d^4$ can be substantially larger than 1.

Further qualitative information can be obtained from eqs. (3.7) for the mixing angles. For $i = 1, 2$, given the very large values of the $\langle \hat{Y}_u \rangle_i$, one can expect vanishingly small left- and right-sector mixing angles. For the top case, $i = 3$, the left-sector mixing angle is still generally small. In fact, note that the quantities Δ_3^u and $\lambda_u^2 v_R^2 + (\lambda'_u \langle \hat{Y}_u \rangle_3)^2$ are very similar in size, and appear with opposite signs in the numerator of $\tan \theta_{L,3}^u$. On the other hand, in the right-sector case, the $\lambda_u^2 v_R^2$ term appears with reversed sign, and this, depending on the choice of parameters, may result in a non-negligible $\theta_{R,3}^u$.

Fig. 5 illustrates the above considerations more quantitatively. The upper panels show the mixing angles in the left-handed top sector against the M_{W_R} mass, in the parity (left panel) and in the no-parity case (right panel). One can see that mixing in the left-handed sector is always fairly small – taking into account the M_{W_R} bound discussed in sec. 3.2, mixing is such that $\sin(\theta_{L,3}^u) \lesssim 2 \times 10^{-2}$. The corresponding angle in the right-handed sector is displayed in the lower panels for the case of TeV-scale parity (the case of no parity gives similar results). In this case, the amount of mixing is not affected at all by the W_R mass bound, and we typically find $\theta_{R,3}^u \approx 10^\circ$ or larger, as also displayed in the histogram. This implies $\sin(\theta_{R,3}^u) \gtrsim 0.2$, and may lead to potential effects in observables like FCNC top decays such as $t \rightarrow cZ$ and observables sensitive to operators with 4 powers of the top field.

In short, mixing angles anywhere else than in the t_R case are vanishingly small. E.g., for b_L , we find $\sin(\theta_{L,3}^d) \lesssim 2 \times 10^{-3}$. This bound is relevant to effects in observables like V_{tb} and R_b , on which we will be more quantitative in sec. 3.4.1.

3.4.1 Electroweak precision tests

$Z^0 \rightarrow b\bar{b}$

The decay $Z^0 \rightarrow b\bar{b}$ is an example of the prototype process $V \rightarrow f\bar{f}$, with V any of the massive vectors, f any of the fermions in the model, and $m_V \geq 2m_f$. This kind of processes allows to estimate the magnitude of tree-level non-oblique corrections that the model introduces.

The interactions relevant to $Z^0 \rightarrow b\bar{b}$ are those in $\mathcal{L}_{Zbb} \equiv Z_\mu^0 J_Z^\mu$, where J_Z^μ in our case is as follows

$$J_Z^\mu = \frac{g}{c_w} \left(\bar{b}_L \gamma^\mu (T_3^d c_{b_L}^2 - s_w^2 Q_d) b_L + \bar{b}_R \gamma^\mu (-s_w^2 Q_d) b_R \right) + \dots, \quad (3.11)$$

where T_3^d and Q_d are the eigenvalues of the weak isospin τ^3 and electric charge operator of down-type quarks, and dots denote the couplings to fermions other than the b . For ease of readability, we also abbreviate $\cos \theta_{L(R),3}^d = c_{b_{L(R)}}$ and $\sin \theta_{L(R),3}^d = s_{b_{L(R)}}$. Note

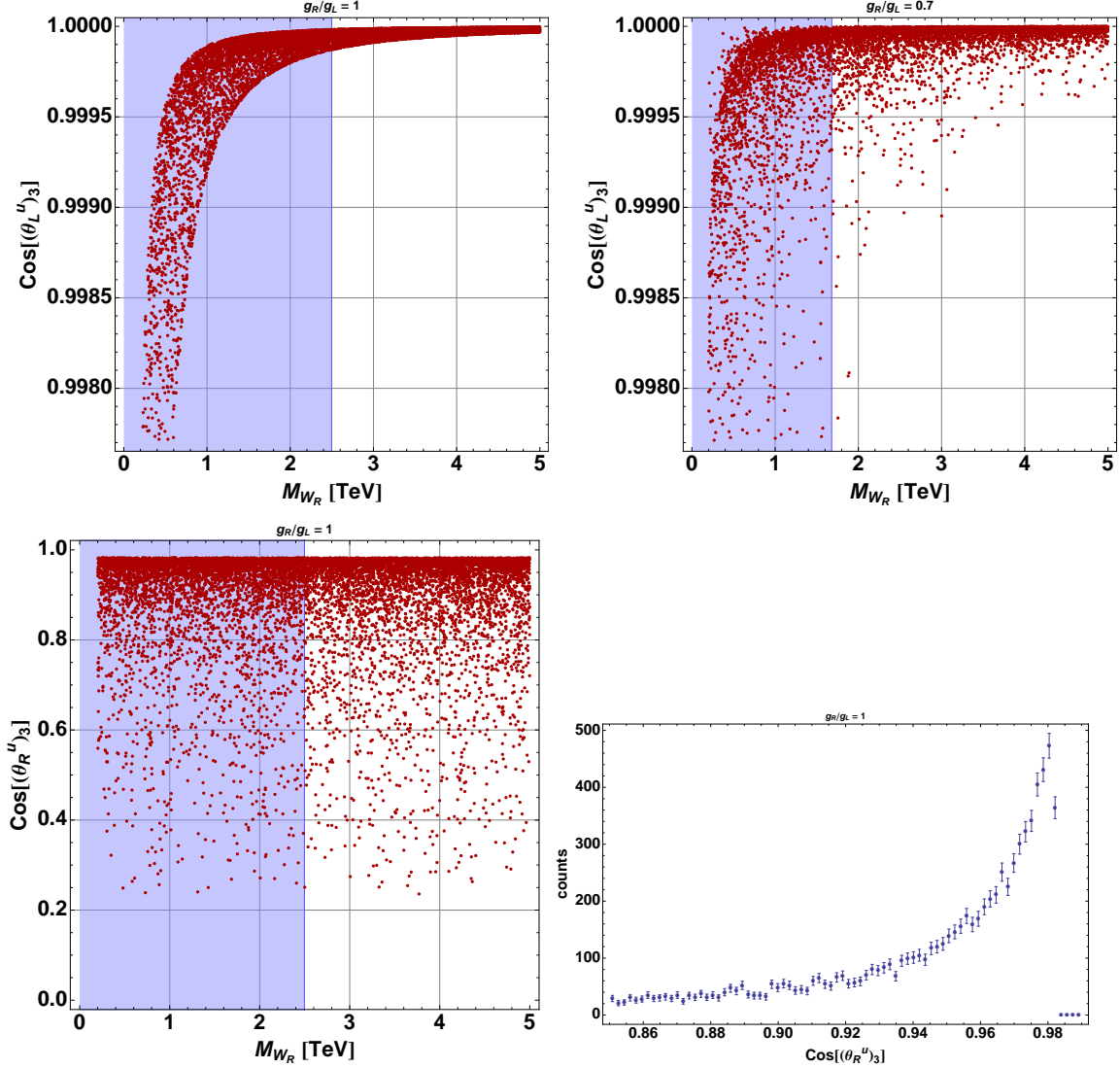


Figure 5: *Upper panels:* M_{W_R} vs. the fermion-mixing angles in the left-handed top sector, for $g_R/g_L = 1$ (leftmost panel) or 0.7 (rightmost panel). *Lower panels:* M_{W_R} vs. the fermion-mixing angles in the right-handed top sector for $g_R/g_L = 1$, and corresponding histogram (see text for further comments).

that the modification with respect to the SM current is only in the left-handed coupling proportional to T_3^d , because the electric charge operator is diagonal across the quark and heavy-fermion fields, hence it commutes with the rotation (3.5). The relevant Lagrangian (3.11) is entirely analogous to that of Ref. [3] hence the correction to $\Gamma(Z^0 \rightarrow b\bar{b})$ in our model will be the same, namely

$$\frac{\delta\Gamma(Z^0 \rightarrow b\bar{b})}{\Gamma(Z^0 \rightarrow b\bar{b})_{\text{SM}}} = -s_{b_L}^2 \frac{2 + 4s_w^2 Q_d}{1 + 4s_w^2 Q_d + 8s_w^4 Q_d^2} + O(s_{b_L}^4). \quad (3.12)$$

To get a numerical idea of the correction implied by eq. (3.12), one can first note that, since s_w^2 is a small number, the coefficient of $-s_{b_L}^2$ is a number close to 2. Then one can recall,

from our previous numerical analysis of fermion mixing, that all the s_{q_i} are tiny in the bulk of the model parameter space. In particular, we quoted $s_{b_L}^2 \lesssim 4 \times 10^{-6}$ in the general discussion of fermion mixing. Therefore, the constraint from $Z^0 \rightarrow b\bar{b}$ plays a completely irrelevant role in our case, in comparison with direct searches of new heavy bosons (we will be back to this later on). In fact, by establishing a lower bound on, e.g., M_{W_R} , these searches constrain the fermion-mixing angles to have values even closer to zero (see again Fig. 5).

We note that, from the above argument, the most interesting effects of decays of the kind $V \rightarrow f\bar{f}$ are expected in the top sector, in particular top production and decays.

Oblique corrections

The S, T and U parameters [14] quantify the modifications in the vacuum polarization diagrams for the $SU(2)_L \times U(1)_Y$ vector bosons, due to the fact that the fermionic currents coupled to them are altered with respect to their SM form. In our model, this occurs because of fermionic mixing and because the new fermions have non-trivial charges under $U(1)_Y$. Following customary notation [15], currents are normalized as

$$J_a^\mu = \sum_f \bar{f} \gamma^\mu T^a f, \quad J_Y^\mu = \sum_f \bar{f} \gamma^\mu Y_f f, \quad (3.13)$$

where T^a denotes the $SU(2)_L$ representation, namely the identity or else $\sigma^a/2$, Y_f the hypercharge assignment for fermion f , and the sum runs over all fermions reported in the table of sec. 2 (our fermion definition includes helicity projectors).

The S and T parameters are defined as [14]

$$S \equiv -16\pi \Pi'_{3Y}(q^2)|_{q^2=0}, \quad T \equiv \frac{4\pi}{s_w^2 c_w^2 M_Z^2} (\Pi_{11}(0) - \Pi_{33}(0)), \quad (3.14)$$

where Π' denotes $d\Pi(q^2)/dq^2|_{q^2=0}$ as usual. Their computation is a simple algebraic problem, after defining the ‘master’ vacuum polarization amplitudes, as the amplitudes with two left-handed currents or respectively one left- and one right-handed current at the two vertices, and fermions of masses m_1, m_2 running in the loop.⁶ These amplitudes are denoted as $\Pi_{LL}(m_1^2, m_2^2, q^2)$ and $\Pi_{LR}(m_1^2, m_2^2, q^2)$, and we shall follow the definition in [15], that we do not rewrite here explicitly.

For the T parameter we find

$$\delta T = \frac{3\pi}{s_w^2 c_w^2 M_Z^2} \left(-2s_{t_L}^2 \Pi_{LL}^{bt} + s_{t_L}^2 (2 - s_{t_L}^2) \Pi_{LL}^{tt} + 2s_{t_L}^2 \Pi_{LL}^{bT} - 2c_{t_L}^2 s_{t_L}^2 \Pi_{LL}^{tT} - s_{t_L}^4 \Pi_{LL}^{TT} \right), \quad (3.15)$$

where δT indicates that we have subtracted the pure SM contribution, obtained in the limit of no fermion mixing. For ease of readability, we have also denoted $\Pi_{LL}(m_X, m_Y, 0) = \Pi_{LL}^{XY}$, and, again, abbreviated $\cos \theta_{L(R),3}^u = c_{t_{L(R)}}$, $\sin \theta_{L(R),3}^u = s_{t_{L(R)}}$.

⁶Specifically, a left- or a right-handed current means an insertion of $i\gamma^\mu \frac{(1\mp\gamma^5)}{2}$ at the vertex, with namely no other overall factor involved, e.g. color factors.

For δS we have instead

$$\delta S = 4\pi \left(-s_{t_L}^2 (2 - 3s_{t_L}^2) \Pi'_{LL}{}^{tt} + 4s_{t_L}^2 \Pi'_{LR}{}^{tt} + 6c_{t_L}^2 s_{t_L}^2 \Pi'_{LL}{}^{tT} - (4c_{t_L}^2 s_{t_L}^2 + s_{t_L}^4) \Pi'_{LL}{}^{TT} - 4s_{t_L}^2 \Pi'_{LR}{}^{TT} \right). \quad (3.16)$$

At this point, we note explicitly that eqs. (3.15) and (3.16) are obtained in the approximation of neglecting fermion mixing other than in the top sector and (this is relevant only for δS) of including in the loops, among the heavy fermions, only the top partner. This is an excellent approximation, given the mass hierarchy among fermionic partners and the size of the mixing angles, discussed before. Both of the δT and δS corrections turn out to depend only on the LH mixing angle $\theta_{L,3}^u$ – in δT the dependence on $\theta_{R,3}^u$ combines in such a way to cancel out in the final result. This fact is very welcome in our case, since, as discussed in sec. 3.4, $\theta_{R,3}^u$ is the only angle sizably different from zero. The allowed experimental values for eqs. (3.15) and (3.16) are of $O(10^{-2})$, with errors of $O(10^{-1})$. Since $s_{t_L}^2$ is about 10^{-3} , even for M_{W_R} as low as 500 GeV, the above corrections, similarly as $\delta\Gamma(Z^0 \rightarrow b\bar{b})$, turn out to play no constraining role at all.

3.4.2 The decay $\bar{B} \rightarrow X_s \gamma$

Similarly as in [3], a further potential constraint for our model implied by flavor mixing comes from the $\text{BR}(\bar{B} \rightarrow X_s \gamma)$, which is very accurately calculated within the SM [16] and also very precisely measured experimentally [17]. The two figures read, respectively (the photon energy cut is in both cases $E_\gamma > 1.6$ GeV.)

$$\begin{aligned} \text{BR}(\bar{B} \rightarrow X_s \gamma)_{\text{exp}} &= (3.55 \pm 0.24 \pm 0.09) \times 10^{-4}, \\ \text{BR}(\bar{B} \rightarrow X_s \gamma)_{\text{SM,NNLO}} &= (3.15 \pm 0.23) \times 10^{-4}, \end{aligned} \quad (3.17)$$

showing very good agreement with each other.

This decay in the SM is generated by a ‘magnetic-penguin’ operator induced by a $W - t_L$ loop. Its Wilson coefficient at the W scale, $C_7(m_t, M_W)$, is modified in our model because the t_L is not a mass eigenstate: $t_L = c_{t_L} \hat{t}_L + s_{t_L} \hat{\psi}_L^t$ (we have again used the shortcut $\cos(\theta_{L,3}^u) = c_{t_L}$). Neglecting the running between the ψ^t mass, here indicated as m_T ($\gtrsim 500$ GeV, as we discussed in sec. 3.4) and the W scale, this effect can be accounted for by a shift in $C_7(m_t, M_W)$,

$$C_7(m_t, M_W) \rightarrow c_L^2 C_7(m_t, M_W) + s_L^2 C_7(m_T, M_W), \quad (3.18)$$

plus an analogous shift in the coefficient $C_8(m_t, M_W)$ of the chromomagnetic penguin operator. Since $C_7(\mu \approx m_b)$ enters as $|C_7|^2$ in the branching ratio, the leading effect is due to interference, and is of $O(s_{t_L}^2)$. To get a numerical idea of the effect, one may use the next-to-leading order (NLO) SM formulae of [18]. Including the shift (3.18) and using $M_T = 500$ GeV, we obtain

$$\text{BR}(\bar{B} \rightarrow X_s \gamma) = (3.2 + 1.3 s_{t_L}^2) \times 10^{-4}. \quad (3.19)$$

In view of the smallness of $s_{t_L}^2$ in the bulk of our parameter space, the above shift is well within the theoretical error.

3.5 Further constraints

3.5.1 Electric dipole moments

After diagonalizing the quark – heavy-fermion mass matrix, all CP violating fermion couplings arise from the Y_u or Y_d vevs. In particular, with our choice of basis in eq. (2.6), they must be proportional to $\langle Y_u \rangle$. One may expect that one-loop diagrams with intermediate gauge bosons (either W_R or the flavor bosons \mathcal{G}_i) and up quarks, and one quark mass insertion, may result in new contributions to the up quark EDM. In the flavor-boson case, using eq. (2.5), it is however easy to convince oneself that the contribution to the EDM must be of the form

$$d_e^u \propto \frac{\lambda_u^2 v_L v_R}{\lambda'} \text{Im} \left(\frac{\lambda^a}{2} V_{\text{CKM}}^\dagger \langle \hat{Y}_u \rangle^{-1} V_{\text{CKM}} \frac{\lambda^a}{2} \right)_{11}, \quad (3.20)$$

with λ^a the Gell-Mann matrices. Similarly as the one-loop SM contribution, the contribution in eq. (3.20) vanishes trivially because of the hermiticity of the matrix on the r.h.s.. A completely similar argument holds of course in the W_R case. Hence new contributions to quark EDMs may arise in our model only at the two-loop level and are therefore very small.

3.5.2 Top quark flavor changing effects

Among the model predictions testable at the LHC are top-quark flavor changing effects, e.g. a modification in the $\bar{t}cG$ coupling. In our model, neutral Higgs interactions do not give rise to any flavor changing effect due to the fact that they are diagonal. However, the flavor gauge boson couplings involve the CKM matrix as well as the flavor generators, both of which can mix generations. We will do a detailed study of these effects in a subsequent paper. Here we simply give an estimate of the dominant contribution to the operator $\bar{t}\sigma_{\mu\nu}cG^{\mu\nu}$ to be of order

$$g_{tcG} \sim \frac{v_L v_R}{16\pi^2 (\langle \hat{Y}_u \rangle_3)^3}, \quad (3.21)$$

which can be estimated to be of order $10^{-3} \left(\frac{\text{TeV}}{\langle \hat{Y}_u \rangle_3} \right)^3 \text{TeV}^{-1}$. Such effects have been looked for at the Tevatron and will be looked for in processes such as $GG \rightarrow t\bar{c}$, $cG \rightarrow t\gamma$, etc. at the LHC [19]. The current Tevatron (DØ) bound on the strength of such operators is $\leq 0.018 \text{TeV}^{-1}$ with a 2.2fb^{-1} dataset [20].

3.5.3 Direct searches

A key feature of models of this kind is the existence of three heavy vectorlike families, which essentially helps to ameliorate the severe FCNC bounds expected on the basis of dimensional analysis. In this section we address the bounds on their masses based on direct collider searches. The CDF collaboration has searched for up-type heavy quarks (called generically t' in the literature) and provides a lower bound on their mass of 335 GeV [21]. Likewise, there is a lower limit on down-type heavy quarks, also from CDF, giving $m_{\psi_d} \geq 385 \text{GeV}$ [22]. These analyses assume the heavy quarks to decay 100% of the time to a W and light quarks. This will hold in our model for the lightest of the vectorlike quarks.

4. Lepton Sector

Within our framework, the discussion of the lepton sector is completely parallel to the quark sector as far as the flavor gauge boson and charged lepton spectra are concerned. The relevant flavor gauge group is in this case $SU(3)_{\ell_L} \times SU(3)_{\ell_R}$, and one introduces two further flavon fields $Y_{\nu,\ell}$, transforming as $(\bar{3}, 3)$ under this group. The gauge invariant Yukawa interaction for the leptons is then completely analogous to eq. (2.1), but for the replacement of quark doublets with lepton ones and heavy quark partners with heavy lepton partners. Of course, the λ and λ' couplings also do not need to be the same as those appearing in eq. (2.1). The fermion mixing argument leading to eq. (2.7) is likewise trivially generalizable to this case, hence for the diagonal elements of $\langle Y_\ell \rangle$ one expects the relation $\langle \hat{Y}_e \rangle : \langle \hat{Y}_\mu \rangle : \langle \hat{Y}_\tau \rangle = m_e^{-1} : m_\mu^{-1} : m_\tau^{-1}$.

4.1 Neutrino masses

Concerning the neutrino sector, after symmetry breaking the mass matrix for $(\nu_{L,R}, \psi_{L,R}^\nu)$ separates into two block matrices involving (ν_L, ψ_R^ν) or (ν_R, ψ_L^ν) . For the first case we have

$$M_{\nu-N} = \begin{pmatrix} 0 & \lambda_\nu v_L \\ \lambda_\nu v_R & \langle Y_\nu \rangle \end{pmatrix}, \quad (4.1)$$

and similarly for the (ν_R, ψ_L^ν) , after exchanging $L \leftrightarrow R$ in the above matrix. As a result, we have two sets of Dirac neutrinos: ν_L pairing with ψ_R^ν and ν_R with ψ_L^ν . In the limit of $\langle Y_\nu \rangle \gg v_R$, the neutrino mass formula reads

$$M_\nu = \frac{\lambda_\nu^2 v_L v_R}{\langle Y_\nu \rangle}. \quad (4.2)$$

It is clear from the above equation that, if v_R and $\langle Y_\nu \rangle$ are in the few TeV range, we need to choose $\lambda_\nu \sim 10^{-6}$ in order to get the right order of magnitude for neutrino masses (in the sub-eV range). Note that already this is an improvement over the SM, where getting Dirac masses of the right order requires the Yukawa coupling to be much smaller (of order 10^{-12}). Furthermore, we need to choose $\langle Y_\nu \rangle$ in such a way as to get the observed large neutrino mixings. As far as the $\psi_{L,R}^\nu$ fields are concerned they will have masses of order of the flavor symmetry breaking scale $\langle Y_\nu \rangle$.

4.2 Constraints

The above setup is subject to various constraints. First, since neutrinos are Dirac fermions, the right-handed neutrinos have W_R -mediated interactions, that can keep them in equilibrium with charged leptons, unless the right-handed interactions are sufficiently weak. Therefore, the model will predict $N_\nu = 6$ at the Big Bang Nucleosynthesis epoch, which is not consistent with our current understanding of Helium, Deuterium and Lithium abundances of the universe [23]. In fact, this leads to a lower bound on the mass of the right-handed W_R 's of order 3.3 TeV [24]. It must however be noted that, if one generates Majorana masses for the ψ_R^ν by adding $SU(3)_R$ sextet Higgs fields with vev, one can lift

the right-handed neutrinos to higher masses and understand the lightness of left-handed neutrino masses via the seesaw mechanism. In this case, there is no lower bound on the W_R mass from Big Bang Nucleosynthesis.

Second, it is interesting to note a recent lower bound on the W_R mass of 1.36 TeV from the CMS experiment at the LHC [25]. This bound directly applies to our model, and in general to models with Dirac neutrinos.

Third, within this generalization of the model, possible constraints on the flavor gauge boson scale may come from lepton-flavor violating (LFV) decays such as $\mu \rightarrow e\gamma$ and $\mu \rightarrow 3e$. The existing limits on these decays can actually be used to estimate a lower bound on the leptonic flavor scale as follows. Formula (4.2) for the Dirac neutrino mass matrix can be trivially inverted to give

$$\langle Y_\nu \rangle = \frac{\lambda_\nu^2 v_L v_R}{M_\nu}. \quad (4.3)$$

This expression can then be rewritten using the formula $M_\nu = U^* \hat{M}_\nu U^\dagger$ (where \hat{M}_ν is the diagonal neutrino mass matrix) as

$$\langle Y_\nu \rangle_{\alpha\beta} = \lambda_\nu^2 v_L v_R \sum_i U_{\alpha i}^* U_{\beta i} m_i^{-1}, \quad (4.4)$$

with m_i the diagonal entries of \hat{M}_ν . The form of $\langle Y_\nu \rangle$ clearly depends on the neutrino mass ordering. Taking for simplicity normal ordering, $m_1 \ll m_2 \ll m_3$, we get the dominant contribution to be

$$\langle Y_\nu \rangle_{\alpha\beta} = \lambda_\nu^2 v_L v_R U_{\alpha 1}^* U_{\beta 1} m_1^{-1}. \quad (4.5)$$

To have an estimate of the typical $\langle Y_\nu \rangle$ size, one may choose $m_1 \sim 0.5 m_\odot \sim 0.005$ eV and use the tri-bi-maximal form for the lepton mixing matrix U . For a TeV v_R , we find $\langle Y_\nu \rangle$ entries of ~ 100 TeV.

We can now provide an estimate of the decay rates for the processes $\mu \rightarrow 3e$ and $\mu \rightarrow e\gamma$. The amplitude for the $\mu \rightarrow 3e$ process arises at the tree level due to flavor diagonal and off-diagonal gauge boson mixing, namely from the terms $\langle Y_\nu \rangle_{11}$ and $\langle Y_\nu \rangle_{12}$. Since neutrino mixings are large, we assume these terms to be of similar size, indicated as \bar{Y}_ν . Hence the amplitude has the form

$$A(\mu \rightarrow 3e) \sim \frac{1}{2\bar{Y}_\nu^2}. \quad (4.6)$$

This relation is nothing but a simplified version of eqs. (3.2). Note, in particular, that the gauge coupling dependence is of course absent, because the flavor-gauge boson masses also scale with it. To translate eq. (4.6) into a branching ratio, one can use the fact that the calculation of $\mu \rightarrow 3e$ is very similar to the well-known calculation of $\Gamma(\mu \rightarrow e\nu_\mu\bar{\nu}_e) \simeq \Gamma_{\mu,\text{tot}}$, but for the replacement of $G_F/\sqrt{2}$ with the amplitude in eq. (4.6). Hence the branching ratio for $\mu \rightarrow 3e$ can be simply estimated as

$$B(\mu \rightarrow 3e) \sim \frac{1}{2\bar{Y}_\nu^4 G_F^2}. \quad (4.7)$$

This can be of order 10^{-12} , like the current experimental limit [26], for $\overline{Y}_\nu \sim 300$ TeV. Because of our assumption of roughly equal entries in the Y_ν vev matrix, the same estimate applies to all the other LFV decays into three charged leptons, such as $\tau \rightarrow 3e$ or $\tau \rightarrow 3\mu$. The limits on these decays are (currently) much weaker [27] and as such satisfied for the above mentioned value of the leptonic flavor scale. The situation may of course change drastically in the event of new data from a super flavor factory.

Turning to the $\mu \rightarrow e\gamma$ decay, it is generated by a loop graph, and its branching ratio can be estimated to be of order $\frac{27\alpha}{16\pi G_F^2 \overline{Y}_\nu^4}$. Given the loop suppression with respect to eq. (4.7), one gets values safely below the current experimental limits [28] for the above choice $\overline{Y}_\nu \sim 300$ TeV.

A final comment is in order. The above discussion about LFV observables was mostly aimed at verifying that reasonable values for the relevant massive parameters of the model do not lead to conflicts with the current LFV bounds. A separate and potentially interesting question not addressed in this paper is whether our setup may explain a positive LFV signal from current or planned experiments. While our arguments, in particular the one following eq. (4.7), suggest a positive answer, a more detailed one requires invoking a specific flavor model to be embedded within our framework.

5. Conclusions

We have examined the possibility of gauged flavor symmetry as a way to explore the origin of quark lepton masses and mixings. As was noted in Ref. [3], in such models there is an inverse correlation between the quark masses and the flavor hierarchy between the gauge boson masses, making it possible to have light enough flavor gauge bosons and enhanced FCNC effects for the third generation. We have worked within the left-right symmetric electroweak group, which seems to provide a number of advantages over the SM gauge group while maintaining this inverse relation. These advantages include a reduction in the number of input parameters, a possible solution to the strong CP problem without the axion (provided parity is also a TeV-scale symmetry), and the possibility of accommodating neutrino masses. For the case where parity is a TeV-scale symmetry, the lower bounds on both the lightest vectorlike fermion mass as well as on the flavor gauge symmetry scale is of about 5 and respectively 10 TeV (see Figs. 4 and 3). On the other hand, if only $SU(2)_R$, but not parity, survives as a good symmetry down to the TeV scale, the lightest phenomenologically allowed vectorlike quark mass could be much lower. The lightest flavor gauge boson mass gets likewise lower. How low one can go down for these masses depends on what one assumes for the difference between the left and the right couplings, which in turn depends on the nature of the UV complete parity-symmetric theory. We have noted the consistency of the model with all the best-known phenomenology, including electroweak precision data. The detailed predictions for the FCNC effects in the third generation case are currently under investigation; here we only made some qualitative comments about top flavor changing effects.

Acknowledgments

DG acknowledges useful discussions with Roberto Contino, Adam Falkowski, Slava Rychkov and Giovanni Villadoro. The authors also acknowledge Giovanni Villadoro for various comments on the manuscript. The work of DG was supported by the EU Marie Curie IEF Grant no. PIEF-GA-2009-251871. The work of RNM was supported by the NSF grant PHY-0968854, and the work of IS was supported by the U.S. Department of Energy through grant DE-FG02-93ER-40762.

References

- [1] F. Wilczek, Phys. Rev. Lett. **49**, 1549 (1982).
- [2] For some of the earliest papers on gauged flavor symmetry, see R. N. Mohapatra, Phys. Rev. D **9**, 3461 (1974); S. M. Barr and A. Zee, Phys. Rev. D **17**, 1854 (1978); C. L. Ong, Phys. Rev. D **19**, 2738 (1979); F. Wilczek and A. Zee, Phys. Rev. Lett. **42**, 421 (1979); J. Chakrabarti, Phys. Rev. D **20**, 2411 (1979); T. Maehara and T. Yanagida, Prog. Theor. Phys. **61**, 1434 (1979); A. Davidson, M. Koca and K. C. Wali, Phys. Rev. Lett. **43**, 92 (1979); J. Chakrabarti, M. Popovic and R. N. Mohapatra, Phys. Rev. D **21**, 3212 (1980).
- [3] B. Grinstein, M. Redi and G. Villadoro, JHEP **1011**, 067 (2010) [arXiv:1009.2049 [hep-ph]].
- [4] A. Davidson and K. C. Wali, Phys. Rev. Lett. **60**, 1813 (1988); K. S. Babu and R. N. Mohapatra, Phys. Rev. Lett. **62**, 1079 (1989); Phys. Rev. **D41**, 1286 (1990).
- [5] J. C. Pati and A. Salam, Phys. Rev. **D10**, 275 (1974); R. N. Mohapatra and J. C. Pati, Phys. Rev. **D 11**, 566, 2558 (1975); G. Senjanović and R. N. Mohapatra, Phys. Rev. **D 12**, 1502 (1975).
- [6] M. A. B. Beg and H. S. B. Tsao, Phys. Rev. Lett. **41**, 278 (1978); R. N. Mohapatra and G. Senjanovic, Phys. Lett. B **79**, 283 (1978).
- [7] K. S. Babu and R. N. Mohapatra, Phys. Rev. D **41**, 1286 (1990).
- [8] D. Chang, R. N. Mohapatra and M. K. Parida, Phys. Rev. Lett. **52**, 1072 (1984).
- [9] W. M. Yang and H. H. Liu, Nucl. Phys. B **820**, 364 (2009); W. M. Yang, arXiv:1011.4573 [hep-ph]; D. Bhowmick, A. K. Ray and S. Raychaudhuri, Int. J. Mod. Phys. A **13** (1998) 3799.
- [10] T. Feldmann, arXiv:1010.2116 [hep-ph].
- [11] M. Bona *et al.* [UTfit Collaboration], JHEP **0803**, 049 (2008) [arXiv:0707.0636 [hep-ph]].
- [12] G. Beall, M. Bander and A. Soni, Phys. Rev. Lett. **48**, 848 (1982); R. N. Mohapatra, G. Senjanovic and M. D. Tran, Phys. Rev. D **28**, 546 (1983); K. Kiers, J. Kolb, J. Lee, A. Soni and G. H. Wu, Phys. Rev. D **66**, 095002 (2002); Y. Zhang, H. An, X. Ji and R. N. Mohapatra, Phys. Rev. D **76**, 091301 (2007); Nucl.Phys.**B 802**, 247 (2008).
- [13] A. Maiezza, M. Nemevsek, F. Nesti and G. Senjanovic, Phys. Rev. D **82**, 055022 (2010).
- [14] M. E. Peskin and T. Takeuchi, Phys. Rev. D **46**, 381 (1992).
- [15] See: M. E. Peskin and D. V. Schroeder, *An Introduction To Quantum Field Theory*, Reading, USA: Addison-Wesley (1995).

- [16] M. Misiak *et al.*, Phys. Rev. Lett. **98**, 022002 (2007) [arXiv:hep-ph/0609232].
- [17] D. Asner *et al.* [Heavy Flavor Averaging Group], arXiv:1010.1589 [hep-ex].
- [18] K. G. Chetyrkin, M. Misiak and M. Munz, Phys. Lett. B **400**, 206 (1997) [Erratum-ibid. B **425**, 414 (1998)] [arXiv:hep-ph/9612313].
- [19] R. A. Coimbra, P. M. Ferreira, R. B. Guedes, O. Oliveira, A. Onofre, R. Santos and M. Won, Phys. Rev. D **79**, 014006 (2009); T. Han, K. Whisnant, B. L. Young and X. Zhang, Phys. Lett. B **385**, 311 (1996).
- [20] V. M. Abazov *et al.* [D0 Collaboration], Phys. Lett. B **693**, 81 (2010) [arXiv:1006.3575 [hep-ex]].
- [21] A. Lister (for the CDF collaboration), presented at ICHEP 2008, arXiv:0810.3349 [hep-ex]; J. Conway *et al.*, CDF public conference note CDF/PUB/TOP/PUBLIC/10110.
- [22] L. Scodellaro (for the CDF collaboration) presented at ICHEP 2010. D. Whiteson *et al.*, CDF public conference note CDF/PHYS/EXO/PUBLIC/10243.
- [23] K. Nakamura *et al.* [Particle Data Group], J. Phys. G **37**, 075021 (2010).
- [24] R. H. Cyburt, B. D. Fields, K. A. Olive and E. Skillman, Astropart. Phys. **23**, 313 (2005).
- [25] V. Khachatryan *et al.* [CMS Collaboration], arXiv:1012.5945 [hep-ex].
- [26] **SINDRUM** Collaboration, U. Bellgardt *et al.*, *Search for the Decay $\mu^+ \rightarrow e^+ e^+ e^-$* , *Nucl.Phys.* **B299** (1988) 1.
- [27] K. Hayasaka, K. Inami, Y. Miyazaki, K. Arinstein, V. Aulchenko, T. Aushev, A. M. Bakich, A. Bay *et al.* [Belle Collaboration], Phys. Lett. **B687**, 139-143 (2010) [arXiv:1001.3221 [hep-ex]]; J. P. Lees *et al.* [BaBar Collaboration], Phys. Rev. **D81**, 111101 (2010) [arXiv:1002.4550 [hep-ex]].
- [28] **MEGA** Collaboration, M. Ahmed *et al.*, *Search for the lepton-family-number nonconserving decay $\mu \rightarrow e + \gamma$* , *Phys. Rev.* **D65** (2002) 112002, [hep-ex/0111030].